Agr. Nat. Resour. 57 (2023) 191–200

AGRICULTURE AND NATURAL RESOURCES

Journal homepage: http://anres.kasetsart.org

Research article

Property enhancement of polylactic acid/thermoplastic starch blend using zeolite 5A incorporation and biaxial stretching process

Porawee Katanyoota, Piyawanee Jariyasakoolroj, Amporn Sane*

Department of Packaging and Materials Technology, Faculty of Agro-Industry, Kasetsart University, Bangkok 10900, Thailand

Article Info

Article history:
Received 2 December 2022
Revised 13 December 2022
Accepted 14 December 2022
Available online 28 February 2023

Keywords:
Packaging,
PLA,
Stretching rate,
TPS,
Zeolite 5A

Abstract

Importance of the work: Blended polylactic acid/thermoplastic starch (PLA/TPS) is a potential material for packaging; however, it still has poor mechanical and barrier properties.

Objectives: To improve the mixing and performance of PLA/TPS blends by incorporation of zeolite 5A (Z5A) and biaxial orientation of the PLA/TPS/Z5A composite.

Materials & Methods: PLA/TPS/Z5A pellets were prepared by melt-compounding using a twin-screw extruder. The composite pellets were converted into a sheet using cast sheet extrusion followed by biaxial stretching into films. The stretching rate was varied (75−150 mm/s). The microstructural, mechanical and gas barrier properties of the stretched films were investigated.

Results: Z5A incorporation and the stretching rate affected the morphology and properties of the stretched films. The presence of Z5A enhanced mixing of PLA and TPS by reducing the TPS dispersed phase size and improving dispersion of TPS in the blend matrix. The biaxial stretching process increased the ordered structure and crystallinity of the PLA in the PLA/TPS/Z5A films. These improvements led to significant increases in tensile strength and the oxygen and water vapor barriers of the PLA/TPS blend up to 100, 90 and 65%, respectively. Increasing the stretching rate from 75 mm/s to 150 mm/s improved the tensile and impact strength by 26% and 22%, respectively.

Main finding: This was the first report of simultaneous biaxial stretching of PLA/TPS/Z5A composite film. The mixing and performance (mechanical and barrier properties) of the blend were substantially improved by compounding with Z5A and biaxial stretching process.

* Corresponding author.
E-mail address: amporn.s@ku.ac.th (A. Sane)

https://doi.org/10.34044/j.anres.2023.57.1.20

Introduction

Biodegradable materials are considered as potential alternatives to reduce plastic waste from single-use packaging, with polylactic acid (PLA) being one of the promising biodegradable polymers commercially produced for packaging application due to its mechanical properties and gas permeability that are comparable to those of conventional polymers (Lim et al., 2008). However, PLA is rather expensive compared to commodity plastics used for packaging application (Awal et al., 2015). Blending with lower-cost materials, such as thermoplastic starch (TPS), is a potentiallymore economical approach to overcome this limitation. Several researchers have investigated the properties of PLA/TPS blends (Li and Huneault, 2011; Yokesahachart and Yoksan, 2011; Bher et al., 2018). However, the phase separation of PLA/TPS blends often occurred due to the different polarities between the PLA and TPS, resulting in poor mechanical and gas barrier properties (Wootthikanokkhan et al., 2012; Yang et al., 2015). More recently, several studies have been published on the miscibility enhancement of polymer blends based on chemical modification (Akrami et al., 2016; Ghari and Nazockdast, 2022) and the incorporation of inorganic fillers (Djoumaliisky and Zipper, 2004; Thipmanee and Sane, 2012; Yimnak et al., 2020; Chongcharoenyanon and Sane, 2021).

Zeolites are nanoporous, crystalline, aluminosilicate particles composed of a three-dimensional structure of SiO_4 and AlO_4 tetrahedra (Yuzay et al., 2010). They have been used as an additive to improve the miscibility of polymer blends (Djoumaliisky and Zipper, 2004; Thipmanee and Sane, 2012; Yimnak et al., 2020). Djoumaliisky and Zipper (2004) reported improved mechanical properties for recycled mixed polyolefins consisting of polypropylene, high-density polyethylene, low-density polyethylene and polystyrene after incorporating activated zeolite (1–2 weight percent; wt%). Thipmanee and Sane (2012) found that adding zeolite 5A (Z5A) improved the mixing between linear low-density polyethylene (LLDPE) and TPS and led to increases in elongation at break and tensile strength of the LLDPE/TPS blend of at least 20%. Yimnak et al. (2020) studied the effect of Z5A on the properties of a polymer blend containing poly(butylene adipate-*co*-terephthalate) (PBAT) and TPS. They found that addition of Z5A (3 wt%) reduced the size and agglomeration of the TPS dispersed domains in the PBAT continuous phase and resulted in improved tensile strength and a better oxygen barrier.

The biaxial orientation (BO) process involves stretching a plastic sheet or film in both the machine and transverse directions. The orientation of polymer chains is controlled by the processing parameters, such as the stretching rate, temperature and draw ratio (Demeuse, 2011). The BO films usually have enhanced optical, gas barrier and mechanical properties (Breil, 2016). BO has been investigated for improving the performance of biodegradable polymers, such as PLA (Tsai et al., 2010; Jariyasakoolroj et al., 2015; Winotapun et al., 2018) and PBAT (Al-Itry et al., 2015; Li et al., 2018). The BO processing parameters (stretching rate, draw ratio, drawing temperature, annealing time and temperature) usually affected the microstructure and property of BO films of conventional polymers. However, only a few works have reported on the effect of BO parameters on biodegradable polymers. Tsai et al. (2010) reported that the crystallinity of BOPLA increased by 17.5 % when using a stretching rate of 25 mm/s, a 3×3 draw ratio and annealing at 100 °C for 30 s. Jariyasakoolroj et al. (2015) reported that the toughness improvement of BOPLA films depended on simultaneous biaxial stretching parameters, including the draw ratio and stretching rate.

To date, few works have been published on the BO of PLA/TPS films (Chapleau et al., 2007; Jariyasakoolroj et al., 2019). Chapleau et al. (2007) reported on BOPLA/TPS films containing a TPS content of 27–60 wt%, prepared using a stretching rate of 1.7 mm/s, drawing temperature of 90 °C and a draw ratio between 2×2 and 6×6. They found that the mechanical properties of the BOPLA/TPS films decreased at least 2-folds compared to BOPLA film when increasing the TPS content from 27 wt% to 60 wt%. Jariyasakoolroj et al. (2019) reported an improved water barrier and better ductility of BOPLA/TPS film when using a stretching rate of 75 mm/s, a draw ratio of 5×5 and a drawing temperature of 90 °C. However, BO films of PLA/TPS composites have not been reported. Furthermore, the combined effects have not been reported of zeolite incorporation and biaxial stretching on the morphology, microstructure and properties of polymer blends.

Therefore, the objective of this work was to improve the mixing and performance of a PLA/TPS blend by the incorporation of zeolite 5A and biaxial orientation of the PLA/TPS/Z5A composite.

Materials and Methods

Materials

Cassava starch (13 weight percent; wt% moisture content) was purchased from Tong Chan Registered Ordinary Partnership (Thailand). Glycerol (99.5% purity) was obtained

from Siam Chemicals Solutions (Thailand). PLA (IngeoTM 4043D) was purchased from NatureWorks (USA). Zeolite 5A (Z5A) with a pore size range of 0.4–0.5 nm was obtained from Thai Silicate Chemicals (Thailand).

Preparation of polylactic acid/thermoplastic starch/zeolite 5A composite pellets

Z5A and PLA were dried in a hot oven at 120 °C for 5 hr and at 50 °C for 24 h, respectively, before melt-compounding using an extrusion process. The TPS was incorporated with Z5A prior to blending with PLA. Initially, the TPS/Z5A pellets were prepared by mixing cassava starch, glycerol and Z5A (ratio of 39.4:10.3:1.0, respectively) using a 20 L mixer (Mitsubishi; Tokyo, Japan) for 30 min. The mixtures were extruded using a twin-screw extruder (LTE-20-40; Labtech Engineering; Samut Prakan, Thailand) at a screw speed of 180 revolutions per minute (rpm) and a temperature range of 90–160 °C and the extrudate was cut into 2.5 mm-length pellets using a pelletizer. Subsequently, the obtained TPS/Z5A pellets were melt-blended with the PLA to a TPS/Z5A weight ratio of 59.4:40.6 using the same twin-screw extruder operated in the temperature range 120–160 °C at a screw speed of 180 rpm. The PLA/TPS/Z5A extrudate was cut into 2.5 mm pellets using a pelletizer.

Preparation of stretched polylactic acid/thermoplastic starch/zeolite 5A films

The PLA/TPS/Z5A pellets were dried in a hot-air oven overnight before being used in the cast sheet extrusion to prepare a sheet with a thickness of 0.5 mm and width of 300 mm using a single-screw extruder equipped with a chill roll set (CF–W400; Chareon TUT; Samut Sakorn, Thailand), at 150–160 °*C and* a screw speed of 45 rpm. The PLA/TPS/Z5A sheets were cut into a square shape with the width of each side of 96 mm. Each sheet was pre-heated at 90 °C for 60 s before simultaneous biaxial stretching to obtain a 30 µm film using a laboratory biaxial stretcher (KARO IV; Bruckner, Siegsdorf, Germany) at a draw ratio of 4×4. The biaxial stretching rate was varied (75 mm/s or 150 mm/s).

Characterization

Scanning electron microscopy

The surfaces of the stretched PLA/TPS/Z5A films were investigated using a scanning electron microscope (Quanta 450; FEI, Eindhoven, the Netherlands) at an accelerating voltage of 10 kV and a magnification of 1500×. Energy dispersive spectroscopic (EDS) analysis of the PLA/TPS/Z5A films was performed for mapping aluminum (Al) and silicon (Si) elements to locate the positions of the Z5A particles in the stretched films using an EDS instrument (Oxford INCA; EDS systems; Abingdon, UK) at an accelerating voltage of 15 kV and a scanning time of 300 s.

X-ray diffraction

X-ray diffraction analysis of the stretched PLA/TPS/Z5A films was performed to determine the crystal structures of PLA, TPS and Z5A using Cu-Kα radiation (D8 Advance; Bruker, Karlsruhe, Germany). The experiments were performed with a scanning range of 5–40° and a rate of 0.02°/s.

Tensile testing

Tensile testing of the stretched PLA/TPS/Z5A films was performed using a universal testing machine (Instron 5565; Instron Corp., Canton, MA, USA) following ASTM D–882 (ASTM International, 2018) in the machine direction. Tensile measurements were conducted with a 5 kN load cell using a crosshead speed of 50 mm/min and a gauge length of 50 mm at room temperature. All samples were cut into a rectangular shape with the width and length of 1 cm and 10 cm. The samples were conditioned at 50% relative humidity (RH) and 23 °C for 2 d prior to measurement. Each sample contained 10 replicates.

Impact testing

The impact strength of the stretched PLA/TPS/Z5A films was measured using a Pendulum Impact Tester (FIT-01; Labthink International, Medford, OR, USA) following ASTM D–3420 (ASTM International, 2021). The stretched films were cut into a square shape with the width of each side of 100 mm. The impact test was performed using a pendulum energy of 2 J with an impact head diameter of 19 mm. Three specimens were tested for each sample.

Oxygen permeability

The oxygen transmission rate (OTR) of the stretched PLA/TPS/Z5A films was determined using an oxygen permeation analyzer (Ox-tran model 2/21; MOCON; Minneapolis, MN, USA) according to ASTM D–3985 (ASTM International, 2017). The OTR values of the stretched films were measured on a surface area of 50 cm^2 and the samples were stored at 50% RH and 23 °C for 2 d before testing. Triplicate measurements of each sample were performed. The oxygen permeability (OP) was calculated using Equation 1 (Ruiz-Cardona et al., 1996):

$$OP = OTR \times l / \Delta p \quad (1)$$

where *OP* is the oxygen permeability measured in cubic centimeters by millimeters per square meter per second per pascal, *OTR* is the oxygen transmission rate in cubic centimeters per square meter per second, *l* is an average film thickness in millimeters and *Δp* is the partial pressure difference of oxygen gas between the two sides of the film measured in pascals.

Water vapor permeability

The water vapor transmission rate (WVTR) of the stretched PLA/TPS/Z5A films was determined using a water vapor permeation analyzer (Permatran model 3/34; MOCON; Minneapolis, MN, USA) according to ASTM F–1249 (ASTM International, 2020). The WVTR values of the stretched films were measured on a surface area of 50 cm^2 and the samples were stored at 50% RH and 23 °C for 2 d prior to testing. Triplicate measurements of each sample were carried out. The water vapor permeability (WVP) was calculated using Equation 2 (Ruiz-Cardona et al., 1996):

$$WVP = WVTR \times l / \Delta p \quad (2)$$

where *WVP* is the water vapor permeability measured in nanogram by millimeters per square meter per second per pascal, *WVTR* is the water vapor transmission rate in nanogram per square meter per second, *l* is the average film thickness measured in millimeters and *–p* is the partial water vapor pressure difference between the two sides of the film measured in pascals.

Statistical analysis

The data were analyzed using one-way analysis of variance followed by Duncan multiple comparison for mean values. All tests were considered significant when $p < 0.05$. The analyses were performed in the SPSS software package (version 19; SPSS Inc., Chicago, IL, USA).

Results and Discussion

Morphology of stretched polylactic acid/thermoplastic starch/zeolite 5A films

The surface morphologies of the stretched PLA/TPS and PLA/TPS/Z5A films compared to their unstretched sheets are shown in Fig. 1. The unstretched blend and composite sheets had a distribution of TPS dispersed domains in the PLA continuous phase. The unstretched PLA/TPS sheet consisted of the PLA continuous phase and an agglomerated spherical TPS dispersed phase, with a size range of approximately 1-8 μm. This microstructure occurred due to the different polarities of hydrophobic PLA and hydrophilic TPS, leading to limited miscibility between PLA and TPS (Martin and Avérous, 2001). After compounding the blend with Z5A, the size of the TPS dispersed phase reduced to approximately 1–6 μm and showed the presence of elongated structures. When the PLA/TPS sheet was simultaneously biaxially stretched at a stretching rate of 150 mm/s, micro-holes appeared on the surface of the stretched film (Fig. 1B), possibly because of the low adhesion between the PLA continuous phase and the TPS dispersed phase was overcome by the stretching force (Samthong et al., 2015). Micro-holes with sizes of approximately 2−13 μm were observed on the surface of the stretched PLA/TPS film. However, for the stretched films made from the PLA/TPS/Z5A composite, there were fewer, smaller micro-holes (approximately 2–7 μm).

EDS analysis was performed to observe the dispersion of the Z5A particles by mapping both the Si and Al elements in the unstretched and stretched PLA/TPS/Z5A samples to determine the locations of the Z5A particles (Fig. 2). Fig. 2A shows that the Al and Si elements were well dispersed in the unstretched PLA/TPS/Z5A sheet, suggesting the even distribution of Z5A in the PLA/TPS matrix. In addition, after biaxial stretching, uniform dispersion was observed of the Z5A particles in the stretched films (Fig. 2B).

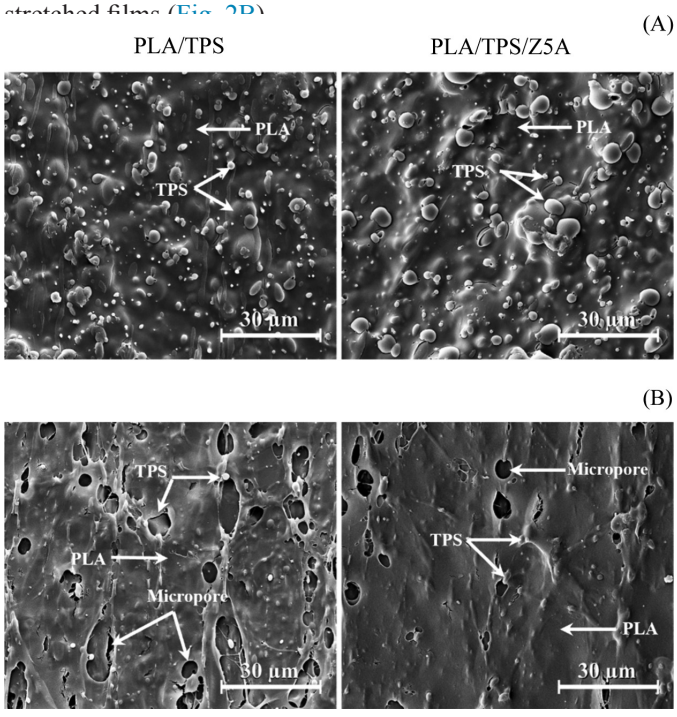

Fig. 1 Scanning electron micrographs: (A) unstretched blended polylactic acid/thermoplastic starch (PLA/TPS) and PLA/TPS/zeolite 5A (Z5A) sheets; (B) stretched PLA/TPS and PLA/TPS/Z5A films prepared at stretching rate of 150 mm/s

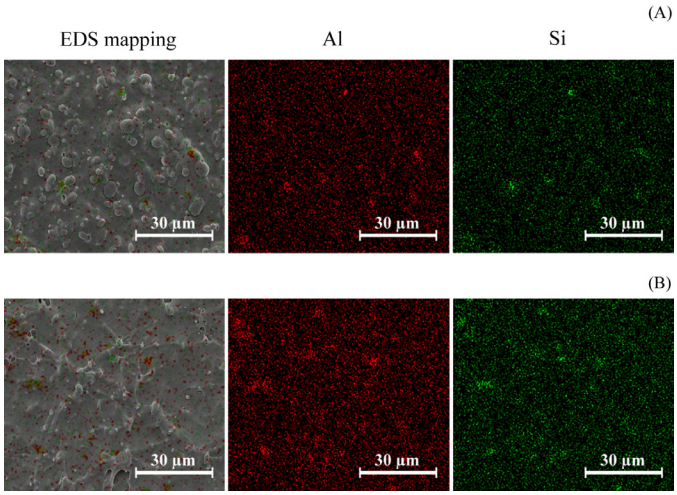

Fig. 2 Energy dispersive spectroscopic elemental mappings of silicon and aluminum: (A) unstretched blended polylactic acid/thermoplastic starch (PLA/TPS)/zeolite 5A (Z5A) sheet; (B) stretched PLA/TPS/Z5A films prepared at stretching rate of 150 mm/s

Microstructure of stretched polylactic acid/thermoplastic starch/zeolite 5A films

Fig. 3 shows the XRD patterns of PLA/TPS and PLA/TPS/Z5A. The XRD patterns of the unstretched PLA/TPS blend and the PLA/TPS/Z5A composite sheet compared with Z5A, PLA and TPS are shown in Fig. 3A. The main characteristic peaks of Z5A appeared at 2θ values of 7.2°, 10.2°, 24.1°, 30.3° and 34.5°. The PLA sheet had a broad diffraction pattern with a 2θ range of 9.5–25°, while TPS had peaks at 2θ = 7.0°, 12.0° and 18.3°, corresponding to the E_H-type structure and at 2θ = 13.2°, 19.5° and 24.5°, corresponding to the V_H-type structure, generated from the complexed formation between amylose and small molecules, such as glycerol (Teixeira et al., 2012). After melt-blending between the PLA and TPS, the obtained PLA/TPS sheet had small characteristic peaks at 18.3° and 19.0°, corresponding to the PLA and TPS crystal structures, respectively, in agreement with the results of Jariyasakoolroj et al. (2019). After incorporation of Z5A, the intensity of peaks at 18.1° and 19.1° became more pronounced, indicating that Z5A acted as a nucleating agent for the PLA/TPS blend. After biaxial stretching, the stretched films of the PLA/TPS blend and the PLA/TPS/Z5A composites showed a sharp peak at 2θ = 16.5–16.7° (Figs. 3B and 3C), indicating the Δ crystal form of PLA, whereas their amorphous part substantially decreased. The results indicated that the PLA crystal structure was intensely induced by the biaxial stretching process (Xu et al., 2020). On the other hand, the XRD peak of TPS was not clearly visible, implying that the crystallization of TPS could be hindered by the presence of PLA (Jariyasakoolroj et al., 2019). When the stretching rate was increased from 75 mm/s to 150 mm/s, the PLA peak at 2θ = 16.5° of the stretched PLA/TPS film became broader due to the presence of smaller crystallites of PLA (as compared in Figs. 3A and 3B). For the stretched PLA/TPS/Z5A films, the PLA peak intensities were lower than that of the stretched PLA/TPS film. However, the area of the amorphous region of PLA was greatly reduced compared to that of the PLA/TPS film. These results suggested that Z5A acted as nucleating agent, inducing heterogeneous nucleation and promoting crystallization of the PLA. In addition, at the stretching rate of 75 mm/s, the peak of the Δ PLA crystal in the composite was at 2θ = 16.5°, with the peak broadening, which implied a decreased crystallite size and increased lattice spacing (Suksut and Deeprasertkul, 2011; Bai et al., 2014). However, with the stretching rate of 150 mm/s, this peak was further broadened and shifted to 2θ = 16.7°. Notably, the addition of inorganic Z5A combined with a sufficiently high stretching rate could induce small PLA crystallites with more compact ordered-structure packing.

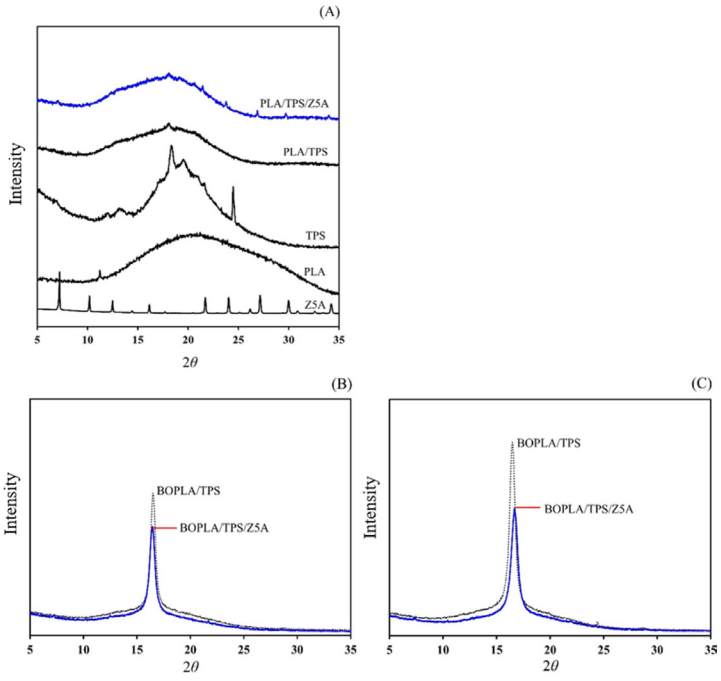

Fig. 3 X-ray diffraction patterns: (A) unstretched polylactic acid (PLA), thermoplastic starch (TPS), PLA/TPS and PLA/TPS/zeolite 5A (Z5A) sheets compared to Z5A; (B) stretched PLA/TPS and PLA/TPS/Z5A films prepared at stretching rate of 75 mm/s; (C) stretched PLA/TPS and PLA/TPS/Z5A films prepared at stretching rate of 150 mm/s, where BO = biaxial orientation

Mechanical properties of stretched polylactic acid/thermoplastic starch/zeolite 5A films

Fig. 4 displays the tensile properties of the stretched PLA/TPS and PLA/TPS/Z5A films compared to those of unstretched sheets. Tensile strength, elongation at break and modulus of the unstretched PLA/TPS sheet were 21.1 MPa, 13.5% and 929.7 MPa, respectively. After incorporating Z5A into the PLA/TPS blend, elongation at break increased to 45.7%, whereas the tensile strength and modulus were not significantly changed. The increase in flexibility of the PLA/TPS/Z5A sheet could have resulted from improved mixing between the PLA and TPS and the uniform dispersion of Z5A in the polymer matrix, as illustrated in Figs. 1 and 2 (Thipmanee and Sane, 2012; Yimnak, et al., 2020). After biaxial stretching, all samples had significantly increased tensile properties, possibly resulting from strain-induced crystallization of PLA in the biaxial stretching process (Jariyasakoolroj et al., 2019; Yoksan et al., 2021). When the stretching rate was increased from 75 mm/s to 150 mm/s, the tensile strength of the stretched PLA/TPS films significantly increased from 30.5 MPa to 37.4 MPa and the modulus increased from 1,598.7 MPa to 1,793.1 MPa. In contrast, elongation at break slightly decreased from 89.4% to 77.9%. For the stretched PLA/TPS/Z5A films, the tensile strength and modulus also increased with the stretching rate, which could be explained by the uniform distribution of Z5A and the functioning of Z5A as a nucleating agent to increase the crystallinity of PLA, in accordance with the XRD results demonstrated in Fig. 3.

Impact strength of stretched polylactic acid/thermoplastic starch/zeolite 5A films

The impact strength values of the stretched PLA/TPS and PLA/TPS/Z5A films are shown in Fig. 5. The impact strength ranges of the stretched PLA/TPS and PLA/TPS/Z5A films were 21.7−22.8 J/mm and 20.8−25.4 J/mm, respectively. Increasing the stretching rate from 75 mm/s to 150 mm/s had no effect on the impact strength of the PLA/TPS films; however, it did increased the impact strength of the PLA/TPS/Z5A films from 20.8 J/mm to 25.4 J/mm. The enhanced toughness of the stretched composite films with increasing stretching speed was consistent with the increase in elongation at break of the stretched PLA/TPS/Z5A films (Fig. 4B), suggesting that the presence of Z5A improved mixing between PLA and TPS and facilitated the crystallization of PLA chains in the stretched composite films, in agreement with the study by Zhao et al. (2022). The trend of increasing toughness of the stretched films with stretching rate agreed with the results reported by Yoksan et al. (2021).

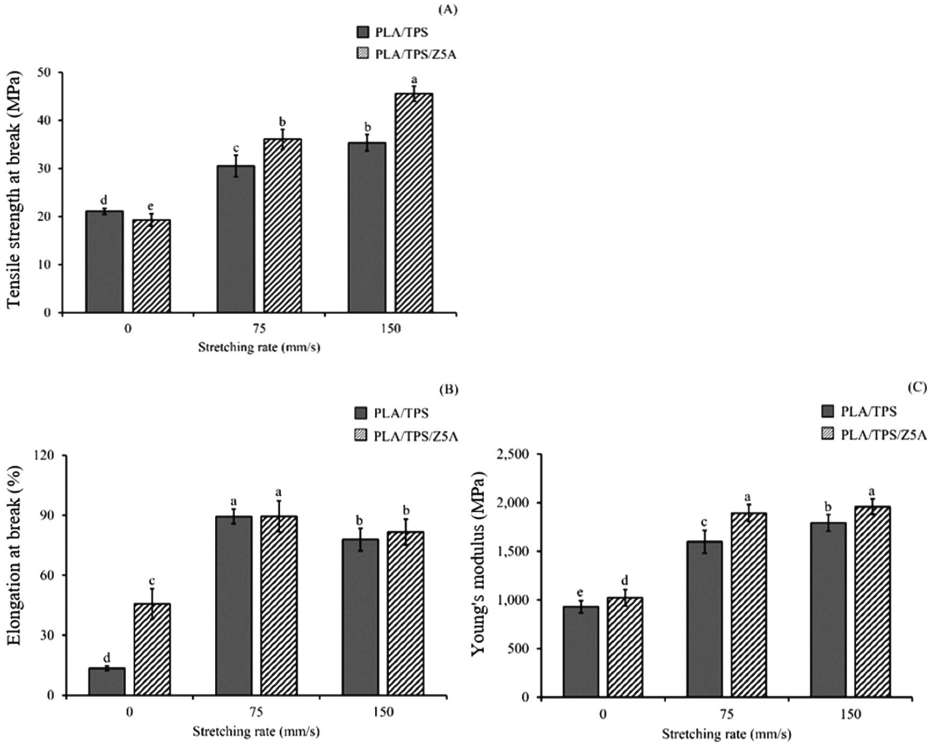

Fig. 4 Tensile properties of stretched blended polylactic acid/thermoplastic starch (PLA/TPS) and PLA/TPS/zeolite 5A (Z5A) films prepared at stretching rates of 75−150 mm/s compared with unstretched sheet: (A) tensile strength; (B) elongation at break; (C) Young's modulus, where different lowercase letters indicate significant ($p < 0.05$) differences and error bars indicate ± SD.

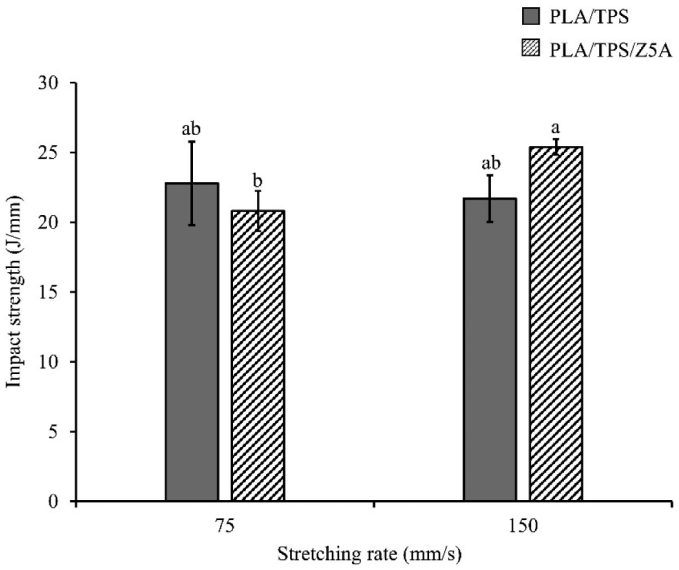

Fig. 5 Impact strength of stretched blended polylactic acid/thermoplastic starch (PLA/TPS) and PLA/TPS/zeolite 5A (Z5A) films prepared at stretching rates of 75−150 mm/s, where different lowercase letters indicate significant ($p < 0.05$) differences and error bars indicate ± SD.

Oxygen permeability of stretched polylactic acid/thermoplastic starch/zeolite 5A films

The OP values of the unstretched sheets and the stretched films of PLA/TPS and PLA/TPS/Z5A are shown in Fig. 6. The OP of the unstretched PLA/TPS sheet was 43.2×10^{-10} cm^3.mm/m^2.s.Pa. After incorporating Z5A into PLA/TPS blend, the OP of unstretched sheet increased to 76.9×10^{-10} cm^3.mm/m^2.s.Pa. The increase in OP could be explained by the porous structure of Z5A with its pore sizes of 0.4–0.5 nm (Baerlocher et al., 2007) being larger than the size of an oxygen molecule (0.35 nm) (Shekhawat et al., 2003), resulting in diffusion of oxygen through the Z5A pores. Other work reported that Z5A could be used for oxygen separation to obtain high purity oxygen (Bastani et al., 2013; Ackley, 2019). After the biaxial stretching process, the OP of stretched PLA/TPS and PLA/TPS/Z5A films decreased at least 90%. Increasing the stretching rate from 75 mm/s to 150 mm/s had no significant effect on the OP of the stretched films, possibly due to the presence of micro-holes in the stretched films (Katanyoota et al., 2022).

Water vapor permeability of stretched polylactic acid/thermoplastic starch/zeolite 5A films

Fig. 7 illustrates the water vapor permeability (WVP) of the unstretched sheets and the stretched films of PLA/TPS and PLA/TPS/Z5A. The WVP of the unstretched PLA/TPS sheet was 42.6×10^{-9} ng.mm/m^2.s.Pa. When Z5A was incorporated into the PLA/TPS blend, the WVP of the unstretched sheet reduced to 33.4×10^{-9} ng.mm/m^2.s.Pa The WVP reduction in the PLA/TPS blend after incorporation of Z5A could

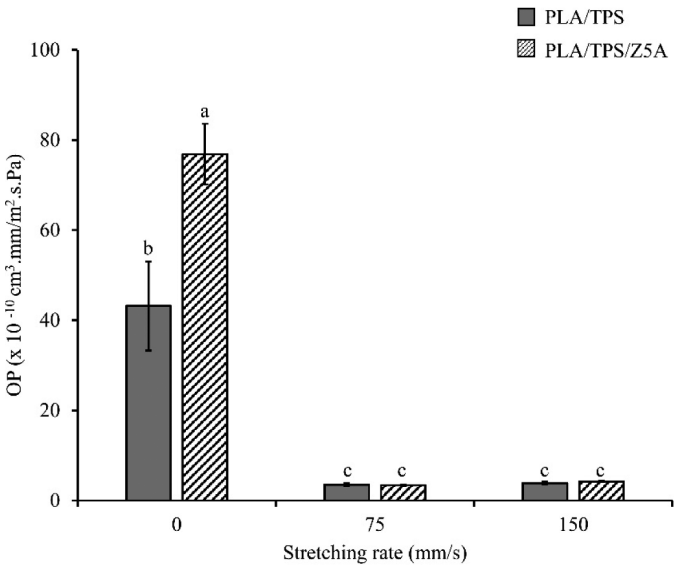

Fig. 6 Oxygen permeability (OP) of unstretched sheets and stretched films of polylactic acid/thermoplastic starch (PLA/TPS) blend and PLA/TPS/zeolite 5A (Z5A) composite prepared at stretching rates of 75−150 mm/s, where different lowercase letters indicate significant ($p < 0.05$) differences and error bars indicate ± SD.

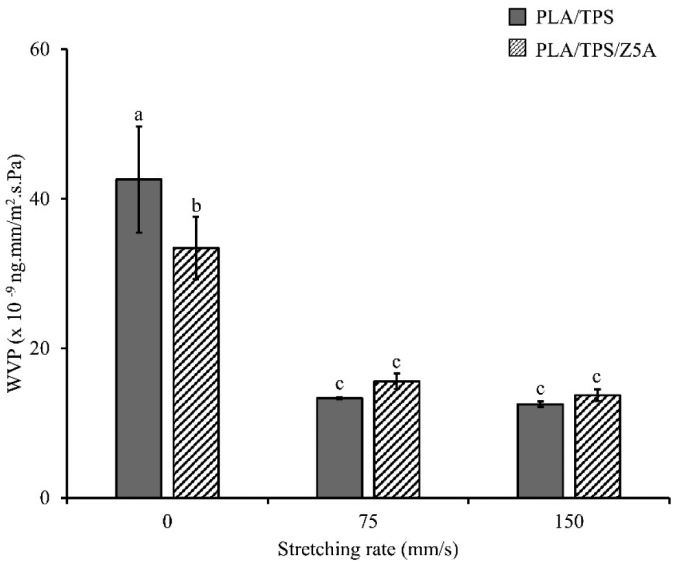

Fig. 7 Water vapor pressure (WVP) of unstretched sheets and stretched films of polylactic acid/thermoplastic starch (PLA/TPS) blend and PLA/TPS/zeolite 5A (Z5A) composite prepared at stretching rates of 75−150 mm/s, where different lowercase letters indicate significant ($p < 0.05$) differences and error bars indicate ± SD

have resulted from Z5A providing a tortuous path, with the increased crystallinity reducing the diffusion rate of the water vapor through the polymer (Ayana et al., 2014; Yimnak et al., 2020; Wongwat el al., 2022). After the biaxial stretching process, the WVP decreased by approximately 55–70%. When the stretching rate increased from 75 mm/s to 150 mm/s, the WVP decreased approximately 10%. The water vapor barrier improvement of the stretched PLA/TPS films resulted from the presence of more-ordered structures from the biaxial stretching process, leading to a reduced rate of water vapor diffusion through the polymer matrix (Delpouve et al., 2012; Jariyasakoolroj et al., 2019). Furthermore, the stretched PLA/TPS/Z5A films had slightly higher WVP values compared to the stretched PLA/TPS film, in agreement with the OP results in Fig. 6.

In conclusion, zeolite 5A incorporation and the biaxial stretching process significantly improved the properties of the tested PLA/TPS blends. Compounding with Z5A enhanced the mixing between PLA and TPS by reducing the size of the TPS dispersed phase and providing a uniform distribution of Z5A throughout the blend matrix. Biaxial stretching greatly improved the tensile properties, as well as the oxygen and moisture barrier of the PLA/TPS blend. The microstructure and mechanical strength (tensile and impact) of the stretched PLA/TPS and PLA/TPS/Z5A films depended on the stretching rate. The increase in stretching rate from 75 mm/s to 150 mm/s increased the ordered structure and crystallinity of the PLA in the stretched blend and composite films. The increment in PLA crystallinity occurred due to the presence of Z5A and the biaxial stretching process, contributing to the increased toughness and barrier properties of the stretched PLA/TPS/Z5A films. Additionally, increasing the stretching rate improved the tensile and impact strength of the stretched PLA/TPS/Z5A films.

Conflict of Interest

The authors declare that there are no conflicts of interest.

Acknowledgements

The authors thank the Thailand Research Fund (TRF) and the National Research Council of Thailand (NRCT) under the Royal Golden Jubilee Ph.D. Program (PHD/0127/2561) for student scholarship. This research project was also financially supported by the NRCT (N25A640017). The authors thank Dr Noppadon Kerddonfag at the National Metal and Materials Technology Center for helpful supervision on the biaxial stretching process.

References

ASTM International. 2017. ASTM D–3985, Standard test method for oxygen gas transmission rate through plastic film and sheeting using a coulometric sensor. https://www.astm.org/d3985-17.html, 5 December 2022.

ASTM International. 2018. ASTM D882–18, Standard test method for tensile properties of thin plastic sheeting. https://www.astm.org/d0882-18.html, 5 December 2022.

ASTM International. 2020. ASTM F–1249, Standard test method for water vapor transmission rate through plastic film and sheeting using a modulated infrared sensor. https://www.astm.org/f1249-20.html, 5 December 2022.ASTM International. 2021. ASTM D–3420, Standard test method for pendulum impact resistance of plastic film. https://www.astm.org/d3420-21.html, 5 December 2022.

Ackley, M.W. 2019. Medical oxygen concentrators: A review of progress in air separation technology. Adsorption 25: 1437–1474. doi.org/10.1007/s10450-019-00155-w

Akrami, M., Ghasemi, I., Azizi, H., Karrabi, M., Seyedabadi, M. 2016. A new approach in compatibilization of the poly(lactic acid)/thermoplastic starch (PLA/TPS) blends. Carbohydr. Polym. 144: 254–262. doi.org/10.1016/j.carbpol.2016.02.035

Al-Itry, R., Lamnawar, K., Maazouz, A., Billon, N., Combeaud, C. 2015. Effect of the simultaneous biaxial stretching on the structural and mechanical properties of PLA, PBAT and their blends at rubbery state. Eur. Polym. J. 68: 288–301. doi.org/10.1016/j.eurpolymj.2015.05.001

Awal, A., Rana, M., Sain, M. 2015. Thermorheological and mechanical properties of cellulose reinforced PLA bio-composites. Mech. Mater. 80: 87–95. doi.org/10.1016/j.mechmat.2014.09.009

Ayana, B., Suin, S., Khatua, B. 2014. Highly exfoliated eco-friendly thermoplastic starch (TPS)/poly(lactic acid)(PLA)/clay nanocomposites using unmodified nanoclay. Carbohydr. Polym. 110: 430–439. doi.org/10.1016/j.carbpol.2014.04.024

Baerlocher, C., McCusker, L.B., Olson, D.H. 2007. Atlas of Zeolite Framework Types. Elsevier. Amsterdam, the Netherlands.

Bai, H., Huang, C., Xiu, H., Zhang, Q., Fu, Q. 2014. Enhancing mechanical performance of polylactide by tailoring crystal morphology and lamellae orientation with the aid of nucleating agent. Polymer 55: 6924–6934. doi.org/10.1016/j.polymer.2014.10.059

Bastani, D., Esmaeili, N., Asadollahi, M. 2013. Polymeric mixed matrix membranes containing zeolites as a filler for gas separation applications: A review. J. Ind. Eng. Chem. 19: 375–393. doi.org/10.1016/j.jiec.2012.09.019

Bher, A., Auras, R., Schvezov, C.E. 2018. Improving the toughening in poly(lactic acid)-thermoplastic cassava starch reactive blends. J. Appl. Polym. Sci. 135: 46140.

Breil, J. 2016. Oriented film technology. In: John, R., Wagner, J. (Eds.). Multilayer Flexible Packaging. William Andrew Publishing. Boston, MS, USA, pp. 153–172.

Chapleau, N., Huneault, M., Li, H. 2007. Biaxial orientation of polylactide/thermoplastic starch blends. Int. Polym. Process. 22: 402–409. doi.org/10.3139/217.2070

Chongcharoenyanon, B., Sane, A. 2021. Effect of overall migration on tensile properties of biobased plastics containing polylactic acid, thermoplastic starch and zeolite. Agr. Nat. Resour. 55: 611–617. doi.org/10.34044/j.anres.2021.55.4.11

Delpouve, N., Stoclet, G.G., Saiter, A., Dargent, E., Marais, S.P. 2012. Water barrier properties in biaxially drawn poly(lactic acid) films. J. Phys. Chem. B 116: 4615–4625. doi.org/10.1021/jp211670g

Demeuse, M.T. 2011. Biaxial Stretching of Film: Principles and Applications. Woodhead Publishing. Cambridge, UK.

Djoumaliisky, S., Zipper, P. 2004. Modification of recycled polymer blends with activated natural zeolite. Macromol. Symp. 217: 391–400. doi.org/10.1002/masy.200451335

Ghari, H.S., Nazockdast, H. 2022. Morphology development and mechanical properties of PLA/differently plasticized starch (TPS) binary blends in comparison with PLA/dynamically crosslinked "TPS+ EVA" ternary blends. Polymer 245: 124729. doi.org/10.1016/j.polymer.2022.124729

Jariyasakoolroj, P., Tashiro, K., Chinsirikul, W., Kerddonfag, N., Chirachanchai, S. 2019. Microstructural analyses of biaxially oriented polylactide/modified thermoplastic starch film with drastic improvement in toughness. Macromol. Mater. Eng. 304: 1900340. doi.org/10.1002/mame.201900340

Jariyasakoolroj, P., Tashiro, K., Wang, H., Yamamoto, H., Chinsirikul, W., Kerddonfag, N., Chirachanchai, S. 2015. Isotropically small crystalline lamellae induced by high biaxial-stretching rate as a key microstructure for super-tough polylactide film. Polymer 68: 234–245. doi.org/10.1016/j.polymer.2015.05.006

Katanyoota, P., Jariyasakoolroj, P., Sane, A. 2022. Mechanical and barrier properties of simultaneous biaxially stretched polylactic acid/thermoplastic starch/poly(butylene adipate-*co*-terephthalate) films. Polym. Bull. 2022: 1–19. doi.org/10.1007/s00289-022-04312-0

Li, H., Huneault, M.A. 2011. Effect of chain extension on the properties of PLA/TPS blends. J. Appl. Polym. Sci. 122: 134–141. doi.org/10.1002/app.33981

Li, J., Lai, L., Wu, L., Severtson, S.J., Wang, W.J. 2018. Enhancement of water vapor barrier properties of biodegradable poly(butylene adipate-*co*-terephthalate) films with highly oriented organomontmorillonite. ACS Sustainable Chem. Eng. 6: 6654–6662. doi.org/10.1021/acssuschemeng.8b00430

Lim, L.T., Auras, R., Rubino, M. 2008. Processing technologies for poly(lactic acid). Prog. Polym. Sci. 33: 820–852. doi.org/10.1016/j.progpolymsci.2008.05.004

Martin, O., Avérous, L. 2001. Poly(lactic acid): Plasticization and properties of biodegradable multiphase systems. Polymer 42: 6209–6219. doi.org/10.1016/S0032-3861(01)00086-6

Ruiz-Cardona, L., Sanzgiri, Y.D., Benedetti, L., Stella, V.J., Topp, E.M. 1996. Application of benzyl hyaluronate membranes as potential wound dressings: evaluation of water vapour and gas permeabilities. Biomaterials 17: 1639–1643. doi.org/10.1016/0142-9612(95)00324-X

Samthong, C., Seemork, J., Nobukawa, S., Yamaguchi, M., Praserthdam, P., Somwangthanaroj, A. 2015. Morphology, structure, and properties of poly(lactic acid) microporous films containing poly(butylene terephthalate) fine fibers fabricated by biaxial stretching. J. Appl. Polym. Sci. 132: 41415. doi.org/10.1002/app.41415

Shekhawat, D., Luebke, D.R., Pennline, H.W. 2003. A review of carbon dioxide selective membranes. A Topical Report. National Energy Technology Laboratory United States Department of Energy. Pittsburgh, PA, USA.

Suksut, B., Deeprasertkul, C. 2011. Effect of nucleating agents on physical properties of poly(lactic acid) and its blend with natural rubber. J. Polym. Environ. 19: 288–296. doi.org/10.1007/s10924-010-0278-9

Teixeira, E.d.M., Curvelo, A.A., Corrêa, A.C., Marconcini, J.M., Glenn, G.M., Mattoso, L.H. 2012. Properties of thermoplastic starch from cassava bagasse and cassava starch and their blends with poly(lactic acid). Ind. Crops Prod. 37: 61–68. doi.org/10.1016/j.indcrop.2011.11.036

Thipmanee, R., Sane, A. 2012. Effect of zeolite 5A on compatibility and properties of linear low-density polyethylene/thermoplastic starch blend. J. Appl. Polym. Sci. 126: E252–E259. doi.org/10.1002/app.36850

Tsai, C.C., Wu, R.J., Cheng, H.Y., Li, S.C., Siao, Y.Y., Kong, D.C., Jang, G.W. 2010. Crystallinity and dimensional stability of biaxial oriented poly(lactic acid) films. Polym. Degrad. Stab. 95: 1292–1298. doi.org/10.1016/j.polymdegradstab.2010.02.032

Winotapun, C., Kerddonfag, N., Daud, W., Chinsirikul, W., Takarada, W., Kikutani, T. 2018. Effect of biaxial-simultaneous stretching conditions on OTR and CO_2 permeation of CO_2 laser perforated poly(lactic acid) film. Packag. Technol. Sci. 31: 545–556. doi.org/10.1002/pts.2381

Wongwat, S., Yoksan, R., Hedenqvist, M.S. 2022. Bio-based thermoplastic natural rubber based on poly(lactic acid)/thermoplastic starch/calcium carbonate nanocomposites. Int. J. Biol. Macromol. 208: 973–982. doi.org/10.1016/j.ijbiomac.2022.03.175

Wootthikanokkhan, J., Kasemwananimit, P., Sombatsompop, N., Kositchaiyong, A., Isarankura na Ayutthaya, S., Kaabbuathong, N. 2012. Preparation of modified starch-grafted poly(lactic acid) and a study on compatibilizing efficacy of the copolymers in poly(lactic acid)/thermoplastic starch blends. J. Appl. Polym. Sci. 126: E389–E396. doi.org/10.1002/app.36896

Xu, S., Tahon, J.F., De-Waele, I., Stoclet, G., Gaucher, V. 2020. Brittle-to-ductile transition of PLA induced by macromolecular orientation. Express Polym. Lett. 14: 1037–1047. doi: 10.3144/expresspolymlett.2020.84

Yang, Y., Tang, Z., Xiong, Z., Zhu, J. 2015. Preparation and characterization of thermoplastic starches and their blends with poly(lactic acid). Int. J. Biol. Macromol. 77: 273–279. doi.org/10.1016/j.ijbiomac.2015.03.053

Yimnak, K., Thipmanee, R., Sane, A. 2020. Poly(butylene adipate-*co*-terephthalate)/thermoplastic starch/zeolite 5A films: Effects of compounding sequence and plasticizer content. Int. J. Biol. Macromol. 164: 1037–1045. doi.org/10.1016/j.ijbiomac.2020.07.169

Yokesahachart, C., Yoksan, R. 2011. Effect of amphiphilic molecules on characteristics and tensile properties of thermoplastic starch and its blends with poly(lactic acid). Carbohydr. Polym. 83: 22–31. doi.org/10.1016/j.carbpol.2010.07.020

Yoksan, R., Dang, K.M., Boontanimitr, A., Chirachanchai, S. 2021. Relationship between microstructure and performances of simultaneous biaxially stretched films based on thermoplastic starch and biodegradable polyesters. Int. J. Biol. Macromol. 190: 141–150. doi.org/10.1016/j.ijbiomac.2021.08.206

Yuzay, I.E., Auras, R., Selke, S. 2010. Poly(lactic acid) and zeolite composites prepared by melt processing: morphological and physical-mechanical properties. J. Appl. Polym. Sci. 115: 2262–2270. doi.org/10.1002/app.31322

Zhao, X., Liu, J., Li, J., Liang, X., Zhou, W., Peng, S. 2022. Strategies and techniques for improving heat resistance and mechanical performances of poly(lactic acid)(PLA) biodegradable materials. Int. J. Biol. Macromol. 118: 115–134. doi.org/10.1016/j.ijbiomac.2022.07.091